JTTEE5 18:572–577
DOI: 10.1007/s11666-009-9370-x
1059-9630/$19.00 © ASM International

Characterization of Plasma-Sprayed Yttria-Stabilized Zirconia Coatings by Cathodoluminescence

Georg Mauer, Doris Sebold, Robert Vaßen, and Detlev Stöver

(Submitted February 25, 2009; in revised form July 2, 2009)

The occurrence of monoclinic zirconia phase has an important impact on the performance of thermal barrier coatings (TBC) of yttria-stabilized zirconia (YSZ). Therefore, a reliable method is needed to detect its contents and to investigate also its spatial distribution within the parent microstructure. This was the motivation to apply cathodoluminescence (CL) spectroscopy. YSZ coatings with different porosities were manufactured by atmospheric plasma spraying. CL analysis yielded monoclinic phase contents of 5.2 ± 1.6% for the high-porous sample and 3.4 ± 0.5% for the low-porous sample. The results were qualitatively confirmed by x-ray diffraction (XRD). However, due to its lower detection sensitivity the XRD results are quantitatively on lower level. Owing to its synthesis method, the applied powder feedstock showed a considerable content of monoclinic phase. The lower the particle temperatures were the larger fraction of monoclinic phase remained untransformed. This has to be considered when spraying high-porous TBCs.

Keywords cathodoluminescense, monoclinic phase, plasma spraying, thermal barrier coatings, yttria-stabilized zirconia (YSZ)

1. Introduction

Plasma spraying is a well-known process to apply coatings starting from powdery feedstock. The powder, suspended in a carrier gas, is injected into a plasma gas jet, which is generated by electric arc discharge between the electrodes inside the torch. After being molten and accelerated in the plasma, the powder particles impact the substrate and form the coating. The process can be carried out in atmosphere, inert gas, or vacuum (Ref 1).

The atmospheric plasma spraying (APS) process is advantageous for the deposition of ceramics, particularly oxide ceramic materials, e.g., for thermal barrier coatings (TBCs). Since more than 30 years, plasma-sprayed yttria-stabilized zirconia (YSZ) thermal barriers have been developed for applications in gas turbines. For these coatings, partially stabilizing (Y-PSZ) is preferred exhibiting the metastable retention of the tetragonal phase at room temperature. Hence, the addition of stabilizing oxides like yttria avoids the deleterious volume expansion which takes place at the diffusionless, martensitic-type tetragonal to monoclinic phase change. It is sufficient to exceed elastic and fracture limits and can only be accommodated by cracking (Ref 2, 3).

Thus, monoclinic phase content is not desirable in TBCs. In this regard, plasma spraying is a favorable deposition process as the rapid solidification of the splats maintains the yttria distribution in the tetragonal phase providing its meta-stabilization. However, if certain porosity should be achieved to further decrease the heat flux through the TBC, significant fractions of the sprayed particles are molten only partially or entirely unmolten. Hence, if the feedstock material exhibits monoclinic phase it may remain untransformed and be introduced into the coating. Dependent on the method of YSZ powder synthesis, considerable contents of monoclinic phase are commonly known.

Therefore, a reliable method is needed to detect possible monoclinic zirconia phase content as well as its spatial distribution within the parent structure at a resolution comparable to the microstructural scale. This was the motivation to apply cathodoluminescence (CL) spectroscopy to atmospheric plasma-sprayed YSZ coatings and to compare the results with those obtained by x-ray diffraction (XRD). The work is reported in this paper.

Many materials can luminescence when they are exposed to an electron, x-ray, ion, or photon beam. Generally, luminescence is associated with light emission in the ultraviolet to infrared region and can exhibit both broad and narrow band spectra. Many of the phases occurring in ceramics, glasses, refractory materials, and biomaterials show distinct luminescence properties allowing their rapid identification. Thus, luminescence spectroscopy is particularly important in the characterization of materials that contain significant amounts of foreign phases or impurities (Ref 4).

Georg Mauer, Doris Sebold, Robert Vaßen, and **Detlev Stöver**, Institut für Energieforschung IEF-1, Forschungszentrum Jülich GmbH, 52425 Jülich, Germany. Contact e-mail: g.mauer@fz-juelich.de.

One approach for the use of the luminescence effect is to attach a suitable light detector to a scanning electron microscope (SEM). In this case, the signal detected is called cathodoluminescence. The bombardment of a luminescent material with high energy electrons can initiate the emission of photons by raising electrons from the valence band into the conduction band, leaving behind a gap. When an electron and a gap recombine, the electron returns to its ground state energy level and it is possible for a photon to be emitted.

Referring to zirconia, the emission in the blue-green region has commonly been reported. Different luminogen effects are referred to in literature and their contributions to the overall luminescence are rated inconsistently. While trace impurities like Ti^{4+} ions are assumed to behave as extrinsic luminogen activators (Ref 5), luminescence of zirconia is also attributed to an intrinsic self-activation produced by the asymmetric coordination of oxygen ions around the Zr^{4+} ions in the monoclinic structure as well as by anion-vacancy-type defects in YSZ (Ref 6). It is established that the luminescence properties of the monoclinic zirconia phase are much more intensive than that of the partially stabilized tetragonal or the fully stabilized cubic phase (Ref 7).

2. Experimental

2.1 Coating Preparation by Atmospheric Plasma Spraying

The samples used for this study were coated by APS on a Multicoat facility (Sulzer Metco, Wohlen, Switzerland) with a three-cathode Triplex II gun mounted on a six-axis robot. The feedstock was a commercially available 7YSZ powder (Sulzer Metco 204NS, d_{10} = 16 μm, d_{50} = 57 μm, d_{90} = 95 μm) with a spherical HOSP™ morphology. Among other impurities, it contained 0.12 wt.% TiO_2. The monoclinic zirconia phase content was declared by the manufacturer to be 10 wt.% (XRD analysis).

The coatings were sprayed on 50 × 50 mm^2 mild steel substrates and subsequently stripped in hydrochloric acid. Parts of the freestanding coatings were used for mercury porosimetry and comparative XRD analysis, respectively. The remaining samples were embedded into epoxy resin to prepare metallographic polished cross sections for SEM investigation and CL analysis.

The spray parameters are listed in Table 1. The stand-off distance and current were varied to produce coatings with markedly low (# A2, 11.4%) and high porosity (# A4, 20.7%), respectively. This is achieved by different particle temperature levels. Measurements using the diagnostic system DPV-2000 (TECNAR Automation Ltd., St-Bruno, QC, Canada) yielded mean particle temperatures and standard deviations from counting statistics of 2637 ± 131 °C and 2433 ± 75 °C for the # A2 and # A4 parameter set, respectively. Details on the measurement methodology and accuracy can be found elsewhere (Ref 8).

Table 1 Atmospheric plasma spraying parameters

Sample	# A2	# A4
Stand-off distance	200 mm	250 mm
Current	520 A	480 A
Primary plasma gas	50 slpm Ar	
Secondary plasma gas	4 slpm He	
Powder feed rate	25 g/min	
Carrier gas	1.6 slpm Ar	
Robot speed	500 mm/s	
Spacing between torch passes	2 mm	

slpm, Standard liters per minute

2.2 Cathodoluminescence Analysis

To begin with, the plasma-sprayed sample # A4 was investigated in a Leo1530-Gemini scanning electron microscope equipped with a CL-detector (EMSystems, Salzgitter, Germany) and a solar2 spectrometer (Proscan, Lagerlechfeld, Germany). The acceleration voltage was 15 kV. Figure 1 gives a CL spectrum of a local incidence of monoclinic zirconia as an example. It shows a maximum intensity at a wavelength of 490 nm and is slightly skewed to longer wavelengths. This is in good agreement to CL spectra reported in literature (Ref 5, 7, 9, 10). It is well known that the monoclinic zirconia phase is more luminescent by orders of magnitudes than the tetragonal (Ref 11) and cubic phases (Ref 12). Thus, no other signals could be detected.

A backscattered electron micrograph (BSE, Fig. 2a) as well as a panchromatic (Fig. 2b) and a monochromatic CL-pattern (wavelength 490 nm, Fig. 2c) were taken from the same area of the sample # A4. The panchromatic CL image is almost identical with the monochromatic one at 490 nm, meaning that mainly monoclinic zirconia is detected. Although tetragonal zirconia is also luminescent, the signal of the monocline phase is orders of magnitude more intense. According to this, the further investigations were carried out on a Zeiss Ultra 55 SEM (Carl Zeiss AG, Göttingen, Germany), applying a standard variable pressure secondary electron detector (VPSE) of a Zeiss Supra 35 SEM used as panchromatic CL-detector. Again, the acceleration voltage was 15 kV. The scintillation voltage of the Everhard-Thornley detector was switched off in order to avoid any scatter light. This approach allows a fast and easy imaging of the luminescent monoclinic zirconia.

To quantify the luminescent areas, the CL patterns were analyzed quantitatively by digital image analysis (analySIS 5.0 software, Olympus Soft Imaging System GmbH, Münster, Germany).

2.3 X-Ray Diffraction Analysis

Comparative x-ray analysis was performed on a D4 Endeavor diffractometer (Bruker AXS GmbH, Karlsruhe, Germany) with a 0.5° divergence slit. The measurement conditions were Cu-Kα radiation, acceleration voltage 40 kV, and beam current 40 mA. The step increment was 0.02° and the count time 8 s per step.

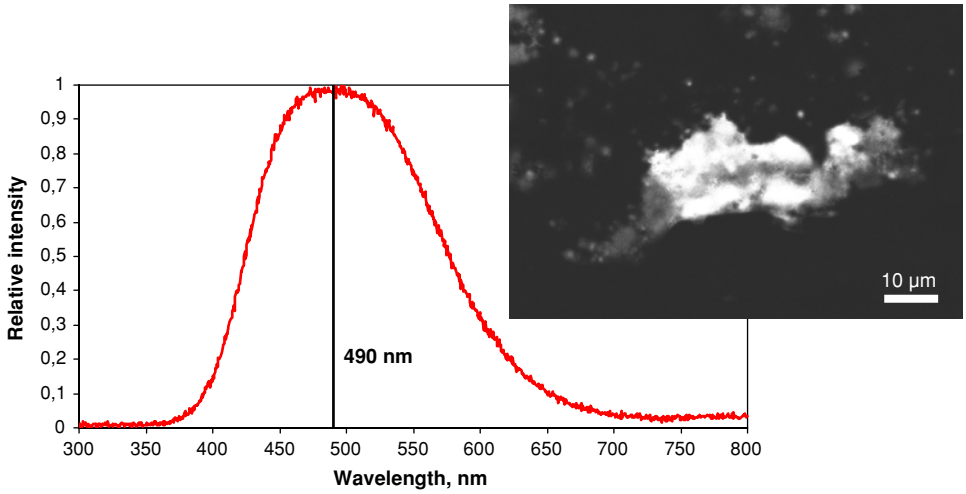

Fig. 1 Cathodoluminescence spectrum of monoclinic phase in a plasma-sprayed YSZ coating. The characteristic wavelength is 490 nm

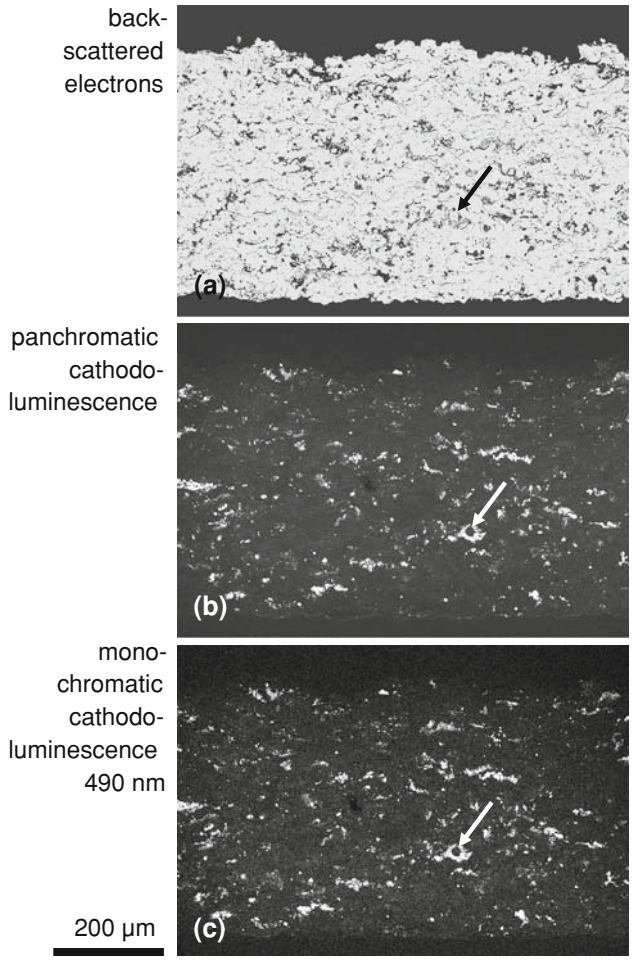

Fig. 2 Backscattered electron (a), panchromatic (b), and monochromatic (c, 490 nm) cathodoluminescence micrographs of the high-porous sample # A4 showing the same display windows. The *arrows* indicate the same structural feature

3. Results and Discussion

3.1 Cathodoluminescence Analysis

In more porous samples, there is a significant higher content of monoclinic zirconia. Image analysis of five CL micrographs per specimen yielded fractions of monoclinic zirconia of 5.2 ± 1.6% for the high-porous sample # A4 and 3.4 ± 0.5% for the low-porous sample # A2. Figure 3 gives the size distribution of cumulative monoclinic zirconia fractions in these specimens. The comparison shows that the distribution in the high-porous sample # A4 is dominated by scattered larger occurrences of monoclinic zirconia extending over more than approximately 10 µm.

Obviously, the reason for this is a larger fraction of partially or nonmolten particles in the higher porous coatings. Investigations on the applied powder feedstock type (Ref 13) showed that in particular the larger particles contain distinct fractions of monoclinic zirconia in total leading up to 15% of the powder volume. It is explained by only partial melting of individual spray dried agglomerates of yttria and unstabilized monoclinic zirconia during the specific production process of the feedstock. To confirm this, the CL analysis of cross-sectioned powder particles is given in Fig. 4. It is obvious that mainly larger and just partially molten particles exhibit monoclinic phase. Hence, such particles can be considered to be the source of the monoclinic zirconia phase content in the sprayed coatings in case they are not completely molten during the spray process.

In Fig. 5, typical morphologies of monoclinic zirconia fractions in the low-porous sample # A2 and the high-porous sample # A4 are shown by backscattering electron and CL micrographs. It becomes clear that areas of unmolten particles and fractions of monoclinic zirconia coincide. The splats of such particles are distributed at random in the sprayed coatings. Thus, spraying

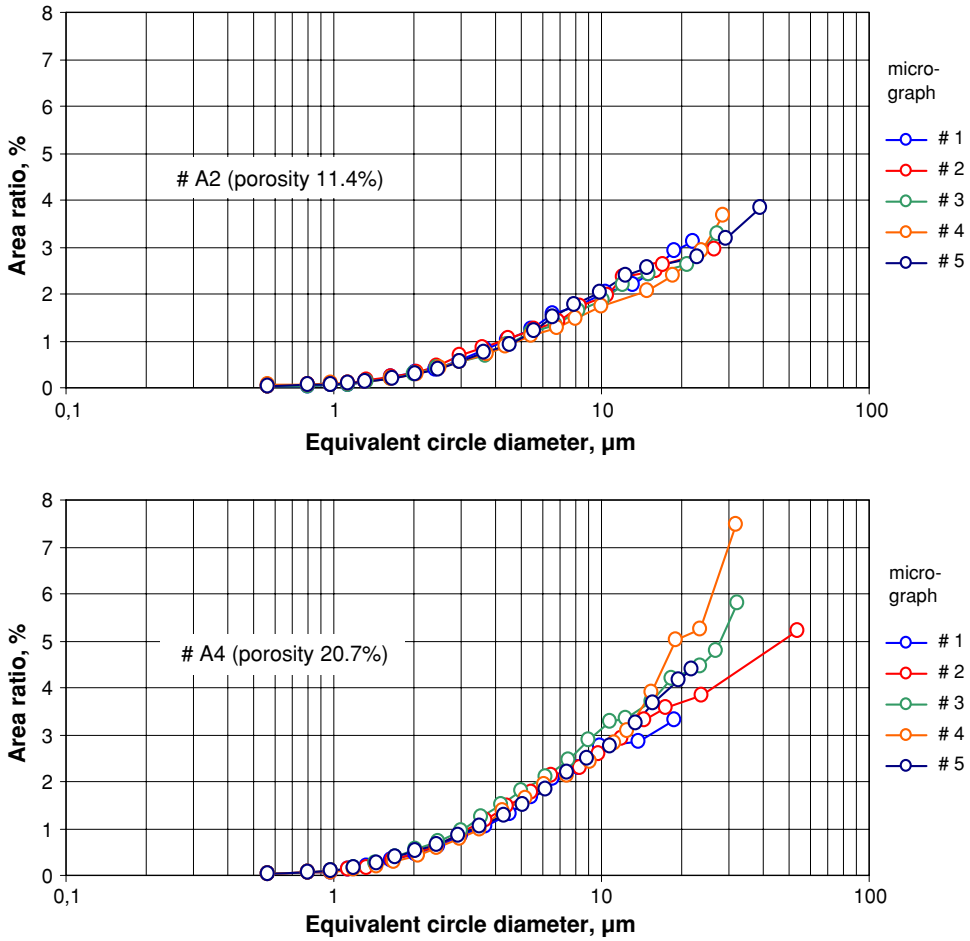

Fig. 3 Size distribution of cumulative monoclinic zirconia fractions in the low-porous sample # A2 (*above*) and the high-porous sample # A4 (*below*) determined in five CL images of each sample

high-porous coatings inducing not or just partially molten particles will inevitably effect an elevated content of unwanted monoclinic zirconia if this phase is already present in the feedstock.

3.2 XRD Analysis

Figure 6 shows the results of comparative XRD analysis of the low-porous sample # A2 and the high-porous sample # A4. The monoclinic phase contents were calculated based on a Rietveld refinement. It is difficult to determine such small contents accurately. However, the results confirm the trend already obtained by CL. In the low-porous sample # A2, a smaller monoclinic content of approximately 1 wt.% could be detected by XRD, in the high-porous sample # A4 it was approximately 3 wt.%, thus being considerably larger.

The comparison emphasizes the advantages of CL microscopy. Obviously the resolution of CL analysis is higher. The detection sensitivity is reported to be up to 10^4 times better than that attainable by XRD enabling the identification of impurity concentrations down to 10^{14} atoms cm^{-3} in good measurement conditions (Ref 14). Moreover, the interesting phases can be clearly localized and associated to microstructural features as the spatial resolution of CL is in the range of 1 µm (Ref 11).

4. Conclusion

Cathodoluminescence is a reliable method to detect unwanted monoclinic zirconia phase content as well as its spatial distribution within in YSZ TBCs at a resolution comparable to the microstructural scale. In this respect, it turned out to be superior to XRD analysis. Applying CL, it was possible to show that areas of partially or entirely unmolten particles and fractions of monoclinic zirconia coincide. Thus, spraying high-porous coatings inducing such unmolten particles will inevitably effect an elevated content of monoclinic zirconia if this phase is already present in the feedstock. Because of its high and local resolution, CL will also give enhanced possibilities to

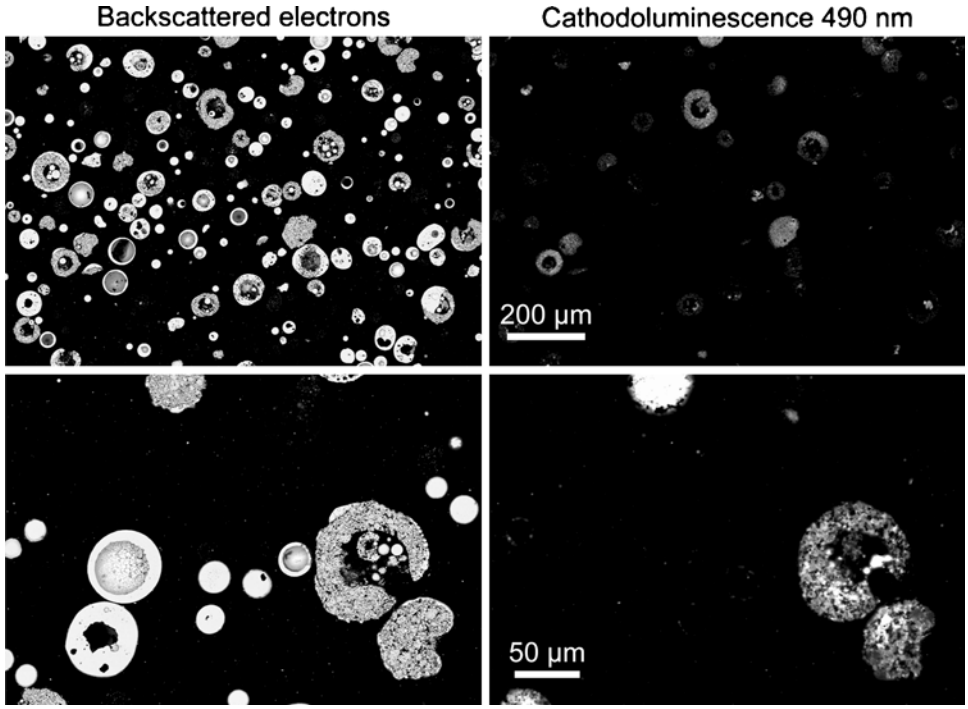

Fig. 4 Occurrence of monoclinic zirconia in cross-sectioned YSZ powder feedstock particles detected by cathodoluminescence. The backscattered electron (*left column*) and cathodoluminescence images (*right column*) show the same display windows

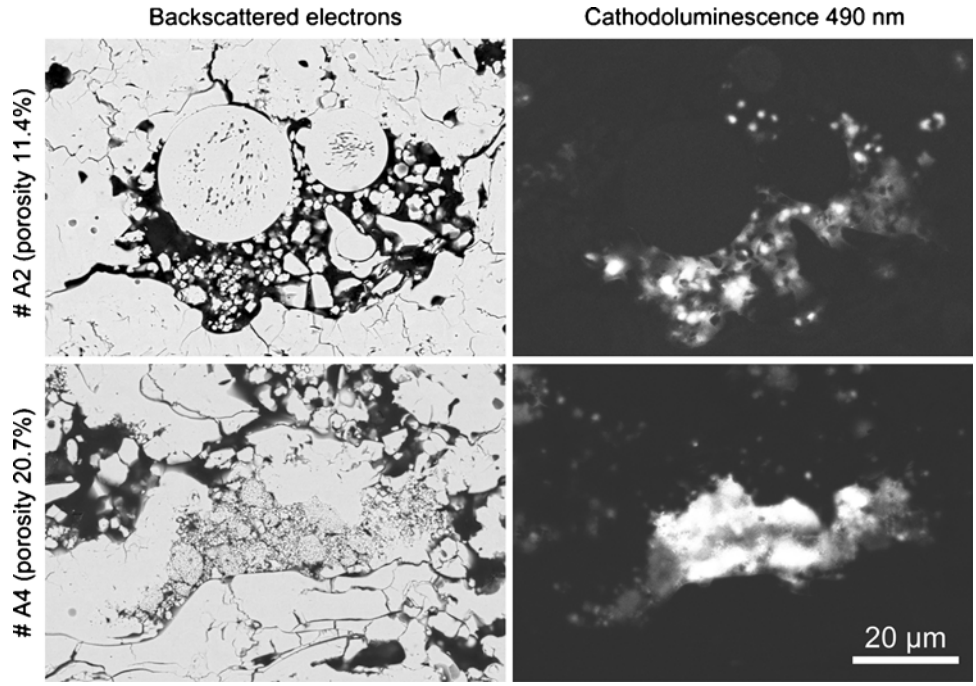

Fig. 5 Typical morphologies of monoclinic zirconia fractions detected by cathodoluminescence in the low-porous sample # A2 (*row above*) and the high-porous sample # A4 (*row below*). The backscattered electron and cathodoluminescence micrographs show the same display windows

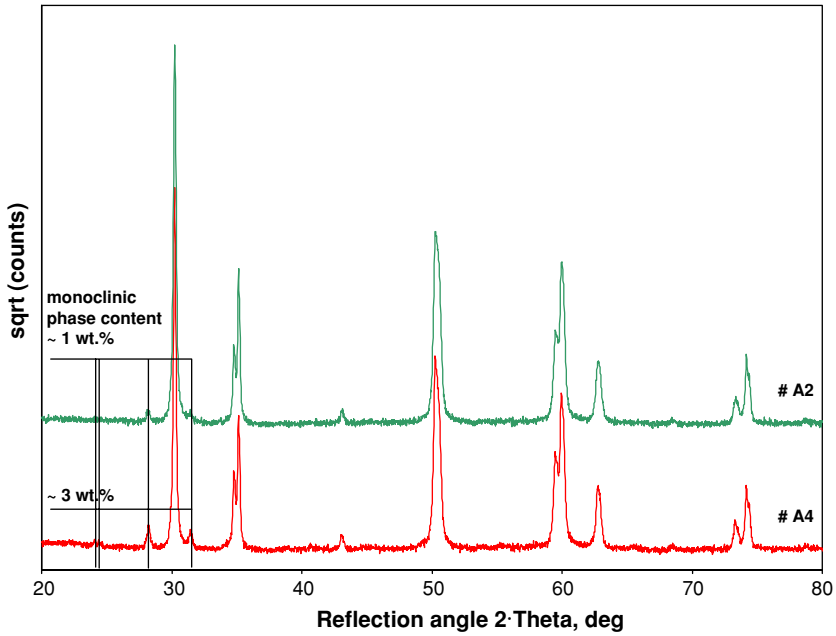

Fig. 6 XRD analysis of the low-porous sample # A2 (*plot above*) and the high-porous sample # A4 (*plot below*). The monoclinic phase contents were calculated based on a Rietveld refinement

investigate the degradation of YSZ TBCs due to phase transformation to the monoclinic phase under high temperature load.

Acknowledgments

The authors gratefully acknowledge the support of Dr. Egbert Wessel (Forschungszentrum Jülich GmbH, IEF-2) who carried out the monochromatic CL analysis as well as useful discussions with Dr. Werner Fischer (IEF-1). Mr. Mark Kappertz (IEF-1) kindly prepared the cross sections of the samples.

References

1. L. Pawlowski, *The Science and Engineering of Thermal Spray Coatings*, Wiley & Sons, Chichester, 1995
2. R. Stevens, *Zirconia and Zirconia Ceramics*, Magnesium Elektron Publication No. 113, Magnesium Elektron Ltd, Manchester, UK, 1986
3. J. Ilavsky, J.K. Stalick, and J. Wallace, Thermal Spray Yttria-Stabilized Zirconia Phase during Annealing, *J. Therm. Spray Tech.*, 2001, **10**(3), p 497-501
4. C.M. MacRae and N.C. Wilson, Luminescence Database I—Minerals and Materials, *Microsc. Microanal.*, 2008, **14**, p 184-204
5. J.T. Sarver, Preparation and Luminescent Properties of Ti-Activated Zirconia, *J. Electrochem. Soc.*, 1966, **113**(2), p 124-128
6. K.A. Shoaib, F.H. Hashmi, M. Ali, S.J.H. Bukhari, and C.A. Majid, Thermoluminescence from X-Ray-Irradiated Stabilized ZrO_2 Single Crystals, *Phys. Stat. Sol. A*, 1977, **40**(2), p 605-612
7. J.T. Czernuszka and T.F. Page, Cathodoluminescence: A Microstructural Technique for Exploring Phase Distributions and Deformation Structures in Zirconia Ceramics, *J. Am. Ceram. Soc.*, 1985, **68**(8), p C196-C199
8. G. Mauer, R. Vaßen, and D. Stöver, Detection of Melting Temperatures and Sources of Errors Using Two-Color Pyrometry During In-flight Measurements of Atmospheric Plasma-Sprayed Particles, *Int. J. Thermophys.*, 2008, **29**, p 764-786
9. M. Karakus and R.E. Moore, CLM—A New Technique for Refractories, *Ceram. Bull.*, 1998, **77**, p 55-61
10. J. Llopis and S.E. Paje, Characterization of Zirconia-toughened Alumina (ZTA) Ceramics by SEM-Cathodoluminescence, *J. Phys. Chem. Solids*, 1993, **54**(8), p 951-954
11. C. Leach and C.E. Norman, Spectroscopic Cathodoluminescence Studies of Mg-PSZ, *J. Mater. Sci.*, 1992, **27**, p 4219-4222
12. G. Koschek and A. Lork, Materials Analysis with Cathodoluminescence Standard Spectra, *Scanning*, 1992, **14**, p 100-103
13. M.J. Lance, J.A. Haynes, M.K. Ferber, and W.R. Cannon, Monoclinic Zirconia Distributions in Plasma Sprayed Thermal Barrier Coatings, *J. Therm. Spray Tech.*, 2000, **9**(1), p 68-72
14. A. Gholinia and C. Leach, Cathodoluminescence Microscopy of Impurity Phases in ZrO_2 Ni Nano-composites, *J. Mater. Sci.*, 1997, **32**, p 6625-6628